UNIVERSITÀ DEGLI STUDI DI GENOVA

DIPARTIMENTO DI SCIENZE DELLA TERRA, DELL'AMBIENTE E DELLA VITA

CORSO DI LAUREA MAGISTRALE IN BIOLOGIA SPERIMENTALE E APPLICATA

CURRICULUM BIOSANITARIO

ANTHRACYCLIN'S EFFECTS ON MITOCHONDRIAL DNA AND BIOGENESIS OF NORMAL CELLS POPULATING THE PERIPHERAL BLOOD OF PATIENTS WITH HODGKIN LYMPHOMA

RELATORI:

GIANMARIO SAMBUCETI

FABIO GHIOTTO

SABRINA CHIESA

CANDIDATO: KAMILA PANA

MATRICOLA: S5674109

Anno Accademico: 2023/2024

TABLE OF CONTENTS

ABSTRACT

Background The preferential accumulation of anthracyclines in the mitochondrial matrix has been proposed to trigger a self-perpetuating vicious cycle with mitochondrial DNA (mtDNA) alteration and oxidative damage enhance one each other leading to a progressive mitochondrial impairment.

Methods To test this hypothesis, we monitored the oxygen consumption rate (OCR) and the mt-DNA copy number (mtDNA-CN) of peripheral blood mononuclear cells (PBMCs) harvested from 23 patients with Hodgkin lymphoma (HL) and negative PET/CT after two ABVD cycles according to the Deauville criteria. In all these patients, PBMCs were isolated at three time points: before treatment (baseline), after two ABVD cycles (interim) and three months after therapy completion (EoT). Baseline data were compared with the corresponding features of 23 subjects selected according to a case-control criterion. Seahorse technology was exploited to evaluate PBMC~~s~~ oxygen consumption rate (OCR) at baseline, after ATP-synthase inhibition with oligomycin, and after blockade of mitochondrial Complexes I and III with rotenone and antimycin. mtDNA-CN was assayed using Digital Droplet PCR, which allows for the absolute and precise quantification of DNA or RNA fragments by partitioning the sample into thousands of droplets, individually amplifying the target fragments, and subsequently analyzing them to determine the exact concentration of nucleic acid molecules in the sample.

Results At baseline, HL PBMCs showed a decreased mitochondrial OCR in both its ATP-linked and ATP-independent fractions. This impairment mismatched a preserved mitochondrial asset, testified by the mtDNA-CN in HL patients and control subjects. At the interim evaluation, both mitochondrial OCR and mtDNA-CN increased in all HL patients. However, in the 18 subjects scored as complete remission by the Lugano criteria

of EoT PET/CT, both variables decreased back to the baseline values. By contrast, in the 5 patients with persistent disease, both mitochondrial OCR and mtDNA-CN remained elevated.

Conclusions HL neoplastic cells and normal elements share a similar sensitivity to doxorubicin toxicity through mechanisms that involve the regulation of mitochondrial function and biogenesis, possibly configuring the metabolic pattern of PBMCs as a possible marker of treatment effectiveness, at least in HL patients.

1. INTRODUCTION

Hodgkin lymphoma (HL) is a type of cancer affecting the lymphatic system and is among the most prevalent cancers in young adults [1]. In the Western world, HL is one of the most frequent types of lymphoma, with an age-adjusted incidence rate of approximately 3 cases per 100,000 people. Most individuals with HL are diagnosed in early adulthood, with another incidence peak occurring at age 60 and above [2]. HL is a B-cell lymphoproliferative disorder, marked by clonal rearrangements of immunoglobulin genes and recurrent genomic abnormalities in Hodgkin Reed-Sternberg cells within a reactive inflammatory environment [2].

In recent decades, treatment advances have made HL curable in over 80% of cases, with unmatched 5-year survival rates. Newly diagnosed patients have a high likelihood of being cured, shifting focus to long-term toxicity concerns, particularly for early- or intermediatestage disease. Clinical trials still aim to improve cure rates for advanced HL, but long-term effects of treatment are a key consideration [3].

The current treatment involves a combination of genotoxic agents such as doxorubicin, bleomycin, vinblastine, and dacarbazine (ABVD), with or without radiotherapy [4]. It is followed by a PET/CT scan using 18F-fluorodeoxyglucose (FDG) (interim PET) [3], [5]. It is now understood that a PET scan conducted after the initial two cycles of ABVD holds significant prognostic value: if the scan is negative and the treatment continues, the likelihood of recovery is very high [5]. If the scan results are positive, it suggests that the patients are not responding adequately to the current therapy. Consequently, there would be a need to switch to a more aggressive treatment regimen, such as BEACOPP, which

includes bleomycin, etoposide, doxorubicin, cyclophosphamide, vincristine, procarbazine, and prednisone [6].

This regimen has proven effective in destroying cancer cells, leading to over 90% of HL patients achieving cancer-free survival at five years. However, this therapy lacks specificity for cancer cells and can cause genetic damage to healthy cells [4].

Despite its marked improvement in curative potential, chemotherapy with anthracyclines is still flawed by a significant risk for severe consequences. Indeed, the survival rate after complete remission is threatened by an increased risk of new independent neoplasms or heart failure, while the quality of life can be compromised in a significant number of patients by the appearance of a cognitive impairment or reproductive deficiency [7], [8].

The initial organ primarily impacted by doxorubicin is the heart, and additionally, it induces harmful effects on the liver, kidneys, reproductive organs, adipose tissue, and brain [9].

Despite the different nature of involved tissues and organs, these complications share a common feature: their incidence increases with elapsing time for months and years after treatment discontinuation. This characteristic indicates an “irreversible” nature of anthracycline toxicity possibly related to a genetic damage. However, the diffuse nature of toxic damage and its high incidence in tissues, the myocardium and the brain, characterized by a slow proliferation is also compatible with the activation of a self-perpetuating vicious cycle leading to a progressive functional deterioration.

Both concepts fit with the notion that anthracyclines are preferentially accumulated in the mitochondrial matrix [10], where they can interact with both cardiolipin and mitochondrial DNA (mtDNA) [11].

The consequent acceleration in the generation of reactive oxygen species [12] [13] has been thus hypothesized to trigger a self-perpetuating vicious cycle in which the mtDNA and the oxidative damage enhance one each other leading to a progressive impairment of mitochondrial bioenergetic power [14].

The mitochondria are highly dynamic organelles that produce over 90% of the cell's chemical energy via respiration [15]. The mitochondria provide most of the cell energy in the form of adenosine triphosphate (ATP) through OXPHOS, which is executed by the electron transport chain (ETC) within the mitochondria [16]. Mitochondria are not just essential in ATP production via OXPHOS; it is also vital in other biosynthetic, bioenergetic and regulatory pathways.

Human mt-DNA is present at high levels (103-104 copies per cell) with a steady state that can vary by tissue type. Although most of the mitochondrial proteins are transcribed in the nucleus, synthesized in the cytosol, and then transported into the mitochondria, the mt-DNA is not non-sense. For example, in human cells, it encodes for 22 tRNAs and two ribosomal RNAs, as well as 13 polypeptides that comprise core subunits of the electron transport chain (ETC) Complex I, III, IV, and V, which are essential for the OXPHOS activity [16].

In the same way of nuclear DNA, mt-DNA is constantly exposed to external and internal noxious agents, like ROS and ultraviolet light (UV) [17]. However, evidence suggests that the mt-DNA is more susceptible to certain stress-induced damages than nuclear DNA due to its proximity to the sites of OXPHOS and lack of the protection by histones [16].

The repair mechanisms of mt-DNA are not well characterized, and the damaged mt-DNA can also be degraded. Repair mechanisms include base excision repair, and direct

reversal, with evidence of mismatch repair and double-strand break repair possibly existing in the human mitochondria [16].

The commonly found pathologies include reduced OXPHOS/ATP synthesis, ROS overproduction, altered calcium homeostasis, and a surge in inflammation [18].

Besides a heavy load of somatic mutations including point mutations, large-scale deletions and insertions accumulated in both the coding and control regions of mt-DNA, its quantitative changes have been frequently identified in various types of diseases [19].

Mitochondrial DNA copy number (mtDNA-CN), a measure of mtDNA levels per cell, while not a direct measure of mitochondrial function, is associated with mitochondrial enzyme activity and ATP production. mtDNA-CN is regulated in a tissue-specific manner and in contrast to the nuclear genome, is present in multiple copies per cell, with the number being highly dependent on cell type [20].

Measurements of mtDNA-CN in blood have been shown to be relevant to a variety of chronic diseases [15]. Variation in mtDNA-CN has been associated with numerous diseases and traits, including cardiovascular disease, chronic kidney disease, diabetes, and liver diseas. Lower mtDNA-CN has also been found to be associated with frailty and all-cause mortality [20].

Various internal and external factors associated with synthesis of ATP demand influence mtDNA CN in nonneoplastic tissue, including cell growth and differentiation, hormone treatment, age, and reaction to oxidative damage, which are thought to play a role in lymphomagenesis [21].

Moreover, there are several reports suggesting the involvement of mitochondrial dysfunction in cancers. When assessing the relationship between cancer and

mitochondria, mtDNA could provide clues and insight into pathogenesis. Specifically, the presence and quantitation of mtDNA by assessing mtDNA CN is frequently assayed to determine a cell's response to external factors [22].

Previous studies have also revealed that altered mtDNA content in tumor tissues was associated with tumor stage, prognosis, and treatment response, again in a cancer type-specific manner [23].

While some types of cancer cells exhibit decreased mtDNA CN, lymphoma and certain leukemia cells are typically associated with increased mtDNA CN [24]. Indeed, it is noteworthy that cells from patients with chronic lymphocytic leukemia (CLL) Burkitt lymphoma,10 and Epstein-Barr virus (EBV)– transformed lymphoblastoid cell lines showed increased mt-DNA copy number [21].

MtDNA-CN levels can be readily measured in extracted DNA from peripheral blood or other tissues, although in practice most measurements are performed in peripheral blood due to ease of accessibility.

An accessible approach to test this hypothesis is represented by the heterogeneous population of peripheral blood mononuclear cells (PBMCs). PBMCs support to immune function already triggered a wide literature on the metabolic features and mitochondrial respiration of these cells in several disease conditions including cancer and chemotherapy [25].

Accordingly, the present study aimed to verify the response of mitochondrial respiration to doxorubicin (DXR) treatment for HL. These functional analyses were thus complemented with the evaluation of mtDNA copy number to verify whether mitochondrial dynamics and function of "normal" PBMCs are simultaneously affected

by chemotherapy and whether their response is related to treatment effectiveness. This evaluation was performed in HL patients as a clinical model allowing a serial evaluation of DXR effect, and standard criteria to define the treatment effectiveness using PET/CT scanning at well-established time-points.

2. Materials and Methods

2.1. Patient population

The study included 23 patients admitted to the San Martino Polyclinic Hospital of Genoa for suspected, and subsequently confirmed, HL from June 2020 up to January 2023. Control subjects (n = 23) were enrolled from normalcy database collected from our institute in the Preventive Medicine Program. Exclusion criteria were positivity for HBV, HCV and HIV or any other coexistent disease asking for pharmacological therapy. All participants provided their written informed consent to participate in this study that was approved by the Ethical Committee of Regione Liguria. According to current guidelines [26], all patients were submitted to a staging PET/CT imaging of 18F-Fluorodeoxyglucose (FDG) uptake just prior to start of treatment with doxorubicin, bleomycin, vinblastine, and dacarbazine (ABVD) administered at standard doses. FDG imaging was repeated after two ABVD cycles (interim-PET) as well as three months after the end of therapy (EoT-PET).

The interim PET was evaluated according to the Deauville criteria [27] to enroll only patients with a score 1 to 3 in whom the maintenance of ABVD regimen was indicated. The EoT-PET was analyzed according to the Lugano criteria to identify responders and non-responders [28].

2.2 PBMCs Isolations

Blood cell count was assayed according to the same routine procedure of the Institute for both HL patients and control subjects. Sampling was performed at the scheduled time in control subjects. In HL patients, samples were harvested at the three time points of imaging, just before the FDG administration, and thus before treatment start, at interim and EoT.

At the time of blood sampling, further 15 mLs of blood were collected and transferred into the laboratory to be analyzed within 24 h. According to validated procedures [29], PBMCs were isolated using lympholyte gradients (Cedarlane), washed three times with Ca2+/Mg2+ free phosphate-buffered saline (PBS) and resuspended at 5 × 106 cells/mL. Obtained cells were divided and dedicated to the different experimental evaluations.

2.3 Flow Citometry Analysis

The protocol involves preparing a mixture containing 32 µL of dedicated antibodies and 68 µL of Brilliant Buffer. The mixture consists of : 3 ul of BV421 Mouse Anti-human CD4, 3 ul of FITC Anti-human CD3, 3 ul PE Mouse Anti-human CD14, 5 ul of BB700 Mouse Anti-human CD56, 3 ul of APC Mouse Anti-human CD8, 5 ul of Pe-Cy7 Mouse Anti-human CD19, 2 ul of Alexa Fluor 700 Mouse Anti-human CD16, 2 ul of APCvio 770 CD45, 3 ul of BV605 HI100 Hu CD45RA, 3 ul of PE- CF594 Hu CD197. This 100 µL mixture was then combined with 100 µL of whole blood and incubated for 15 minutes at 4°C. Subsequently, 800 µL of 1X Lysis Buffer was added, and the cell suspension was incubated in the dark for 10 minutes at room temperature. At the end of the procedure, the tube was placed into the flow cytometer for acquisition. Data were acquired on a FACS Symphony (Becton Dickinson, Milan, Italy) and data analysis was performed with FlowJo software. The analysis was restricted to viable whole blood, after gating procedures based on forward- and side-scatter features []. In a subset of five control subjects and eight HL patients, the recovery of lymphocytes and monocytes in the expected gate was confirmed by staining with CD3, CD19 and CD14 (Miltenyi Biotec, Bergisch Gladbach, Germany). Cellular viability was evaluated by propidium iodide (PI) exclusion assays. Cells were stained with 1 µg/mL PI (Enzo Life Sciences, Milan, Italy) and PI fluorescence measured after 5 min.

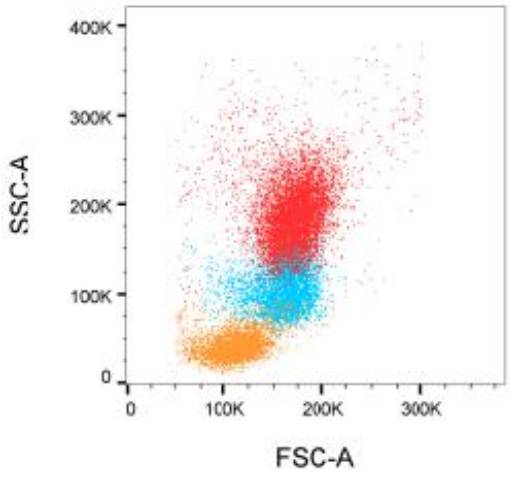

Figure 1

The image shows the gating strategy used for the characterization of various leukocyte populations based on forward and side scatter characteristics. Specifically, three populations are represented: granulocytes (in red), monocytes (in light blue), and lymphocytes (in orange).

2.4 Seahorse Analysis

For this set of experiments, 105 PBMCs were seeded in each of five wells of the Seahorse XFp Extracellular Flux Analyzer (Agilent Technologies, Santa Clara (CA) US) cell plates and gently centrifuged with no brake at 40× g for 3 min. The plate was then rotated 180° before a further centrifugation at 80× g for 3 min to encourage adhesion to the plate and to obtain an evenly dispersed monolayer [30]. Cells were then incubated at 37 °C for 45 min in no-CO2 incubator with Agilent Seahorse DMEM, pH 7.4, enriched with glucose (11 mM).

The method was used to estimate the oxygen consumption rate (OCR) and extracellular acidification rate that was converted to proton efflux rate (PER) using WAVE software (Version 2.4, Agilent), after evaluating the buffer factor of the medium. PER value was divided by 2, to estimate glucose flux through glycolysis (nanomoles × min−1 /million cells).

OCR and ECAR were monitored according to the manufacturer instructions. Briefly, three measurements of OCR and ECAR were taken under control conditions and after sequential injections of 1.5 μM oligomycin (ATP-synthase inhibitor) and 0.5 μM rotenone (Complex I inhibitor) plus 0.5 μM antimycin A (Complex III inhibitor).

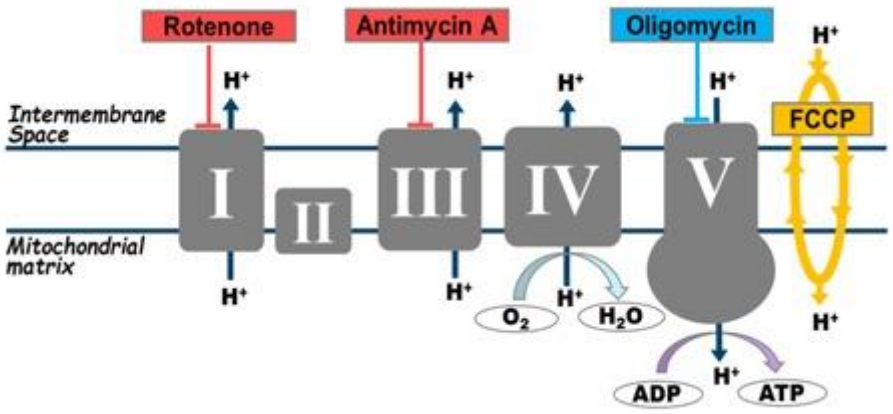

Figure 2

The image represents the mitochondrial complexes of cellular respiration and the agents used for their inhibition. Rotenone acts on complex I, blocking respiration, as does Antimycin A which acts on complex III and Oligomycin which blocks complex V.

2.5 Mitochondrial DNA extraction

Total DNA, including mtDNA, was extracted from the PBMC using QIAamp DNA Kit (Qiagen, Hilden, Germany). DNA concentration was assessed by Qubit Fluorometer using dsDNA HS Assay Kit (ThermoFisher Scientific, San Jose, CA, USA). The mean mtDNA copy number per cell was determined by QX200 droplet digital PCR (ddPCR) system (Bio-Rad, Hercules, CA, USA) using a previously described multiplexing strategy [31]. Were employed two custom FAM-labeled assays targeting mtDNA genes (i.e., mitochondrially encoded NADH dehydrogenase 1, ND1 (dHsaCNS669425578) and DN6 (dHsaCNS941916401)) normalized against two HEX-labeled assays targeting nuclear DNA (i.e., ribonuclease P/MRP subunit p30, RPP30 (dHsaCP2500350) and argonaute RISC component 1, AGO1 (dHsaCP1000002)).

Due to the higher mtDNA copy number compared to nuclear DNA, the two mitochondrial assays (ND1 and DN6) were evaluated in two separate reactions and then averaged. Briefly, 0.9 ng of total DNA was amplified using the ddPCR Supermix for Probes (No dUTP) (Bio-Rad) with the following TaqMan® assays: ND1 or ND6 (900 nM), RPP30 (900 nM), and AGO1 (450 nM) at an annealing/extension temperature of 58°C.

Each sample was run in duplicate with a negative control (no template) and the data analysis was conducted using QuantaSoft™ Analysis Pro software v.1.0.596 (Bio-Rad).

The mtDNA copy number assessment was performed by calculating the ratio between the concentration (copies/µl) of the ND1 or ND6 locus and the mean concentration of RPP30 and AGO1. This ratio was then multiplied by two to account for the presence of two copies of nuclear genes in diploid cells, and the ND1 and ND6 copy numbers were averaged.

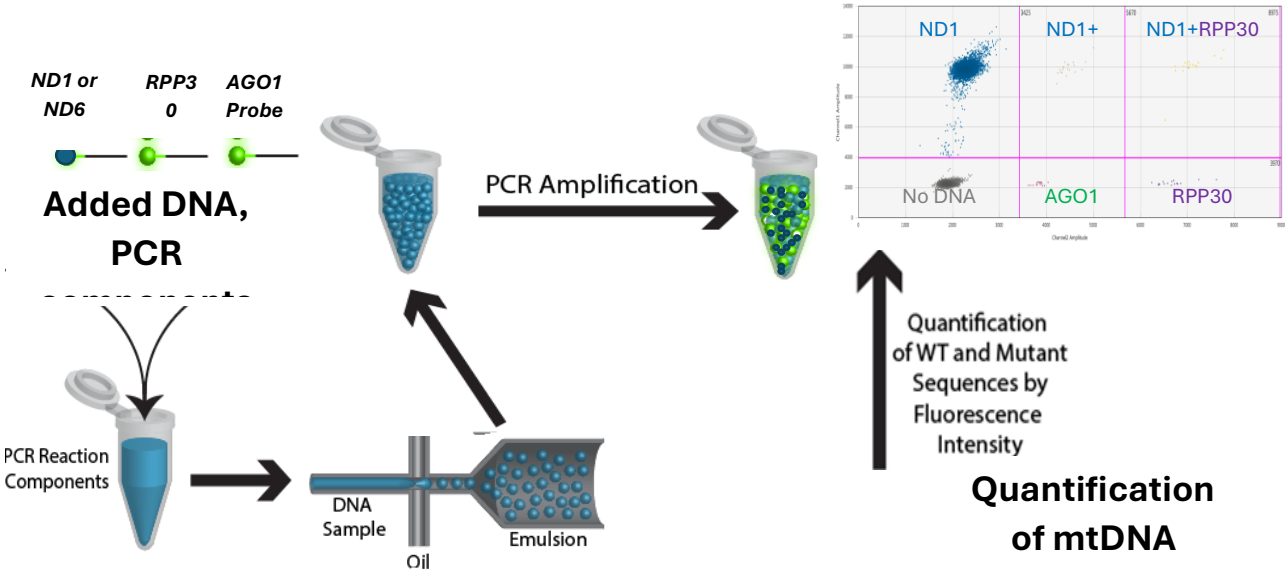

Figure 3 Representation of the technique used for the extraction of mtDNA.

Total DNA, including mtDNA, was extracted from the PBMC using QIAamp DNA Kit (Qiagen, Hilden, Germany). DNA concentration was assessed by Qubit Fluorometer using dsDNA HS Assay Kit (ThermoFisher Scientific, San Jose, CA, USA). The mean mtDNA copy number per cell was determined by QX200 droplet digital PCR (ddPCR) system (Bio-Rad, Hercules, CA, USA) using a previously described multiplexing strategy. Were employed two custom FAM-labeled assays targeting mtDNA genes (i.e., mitochondrially encoded NADH dehydrogenase 1, ND1 (dHsaCNS669425578) and DN6 (dHsaCNS941916401)) normalized against two HEX-labeled assays targeting nuclear DNA (i.e., ribonuclease P/MRP subunit p30, RPP30 (dHsaCP2500350) and argonaute RISC component 1, AGO1 (dHsaCP1000002)). Due to the higher mtDNA copy number compared to nuclear DNA, the two mitochondrial assays (ND1 and DN6) were evaluated in two separate reactions and then averaged. Briefly, 0.9 ng of total DNA was amplified using the ddPCR Supermix for No dUTP) (Bio-Rad) with the following TaqMan® assays: ND1 or ND6 (900 nM), RPP30 (900 nM), and AGO1 (450 nM) at an annealing/extension temperature of 58°C.

2.6 Statistics

All data were reported as mean of ± standard deviation. Unpaired t test was used to compare data between control subjects and HL patients at the first examination. Response of sample cell composition, energy metabolism, mtDNA copy number at the tree time point was tested according to one-way or two-way ANOVA as appropriate. All statistical analyses were carried out by using a dedicated software package, GraphPad Prism version 8 (GraphPad, San Diego, CA, USA).

3. RESULTS

3.1. Patient Population

As shown in Table 1, control subjects and HL patients showed comparable age and similar prevalence of female gender. At routine evaluation of peripheral blood, red blood cell counts, and hemoglobin assays reported similar values in the two groups. However, HL patients showed a significantly higher number of white blood cells that mostly involved both neutrophils and monocytes, while lymphocyte counts were comparable in both.

Table 1: Clinical data

	Control Subjects		HL	
Number	23		23	
Age (years)	45.68 ± 14.4	ns	48.9 ± 20	
Female nr (%)	8 (35%)	ns	8 (35%)	
Hemoglobin (g/L)	135.6 ± 14.2	ns	129.5 ± 12.9	
Red blood cells (millions/µL)	4.83 ± 0.28	ns	4.75 ± 0.33	
Platelets (thousands/µL)	312 ± 140	ns	325 ± 130	
White blood cells (thousands/µL)	8.5 ± 2.6	p<0.05	10.1 ± 3.1	
Neutrophils (thousands/µL)	6.01 ± 1.8	p<0.05	7.5 ± 3	
Monocytes (thousands/µL)	0.66 ± 0.28	p<0.05	0.85 ± 0.35	
Lymphocytes (thousands/µL)	1.57 ± 0.7		1.51 ± 0.52	
Ann Arbor classification			stage II	10 (43%)
			stage III	5 (22%)
			stage IV	8 (35%)

Table 1 Clinical data

The table shows clinical data comparing 23 patients and 23 controls. The control subjects and HL patients showed comparable ages and similar prevalence of females. As can be seen, the red blood cell count and hemoglobin tests reported similar values in both groups. HL patients showed a significantly higher number of white blood cells, primarily involving both neutrophils and monocytes, while the lymphocyte count was comparable in both groups. According to the Ann Arbor classification, 10 patients were at stage II (43%), 5 patients at stage III (22%), and 8 patients at stage IV (35%)

3.2 HL and PBMCs energy metabolism

With respect to control subjects, the PBMCs harvested from HL patients showed an almost double rate of glycolytic flux (Figure 4A). Although overall OCR was similar in the two groups (Figure 4B), its fate was significantly different. Indeed, PBMCs harvested from HL patients showed a lower rate of oxygen usage by the mitochondria. This impairment involved both ATP linked (Figure 4C) and ATP-independent (Figure 4D) fractions.

Consequently, non-mitochondrial (rotenone/antimycin insensitive) OCR was increased in patients with respect to controls (Figure 4E). These findings thus indicated that the normal PBMCs of HL patients display a measurable impairment in mitochondrial OCR as opposed to an increased extramitochondrial oxygen usage.

The marked acceleration of lactate release might be thus compatible with a compensating role by glycolysis in supporting the energy needs of HL PBMCs.

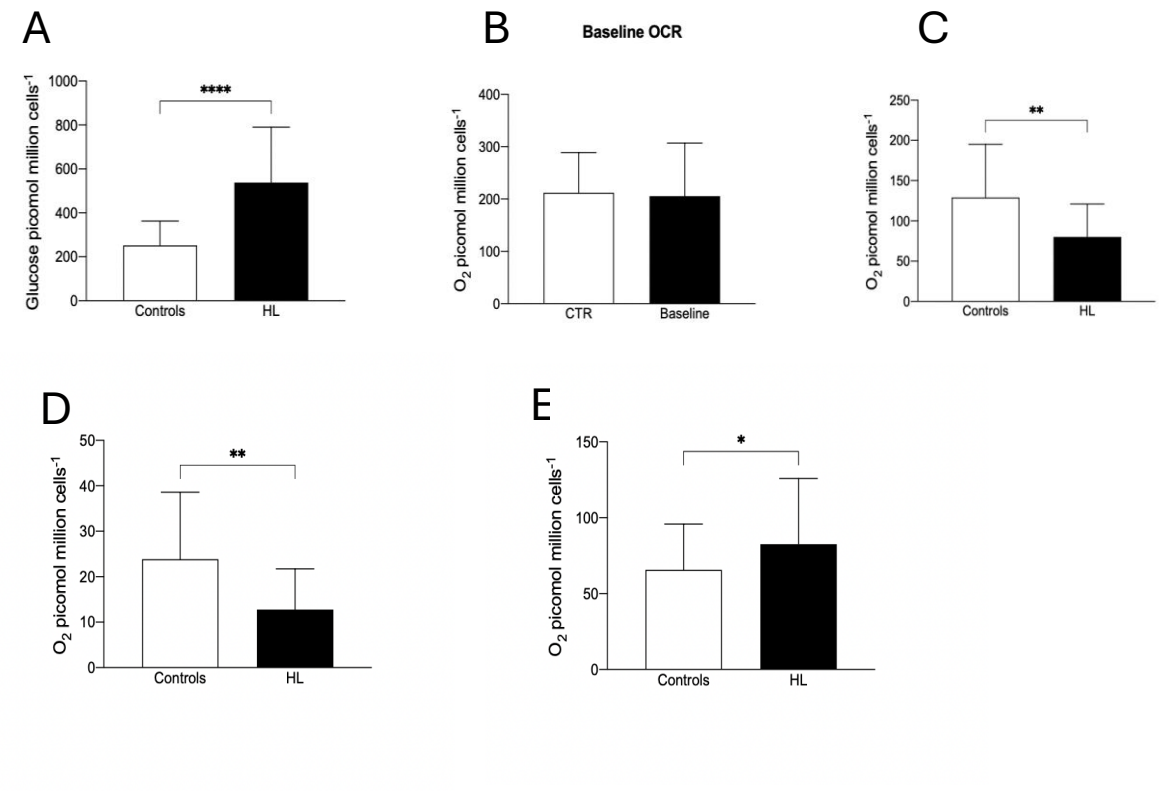

Figure 4 HL and PBMCs energy metabolism results

The figure 4A shows that the PBMCs harvested from HL patients showed an almost double rate of glycolytic flux in comparison to controls. Overall OCR was similar in the two groups (Figure 4B),but its fate was significantly different. Indeed, PBMCs harvested from HL patients showed a lower rate of oxygen usage by the mitochondria. This impairment involved both ATP linked (Figure 4C) and ATP-independent (Figure 4D) fractions. Non-mitochondrial (rotenone/antimycin insensitive) OCR was increased in patients with respect to controls (Figure 4E).

3.3 Chemotherapy and PBMCs energy metabolism

Average glucose consumption (Figure 5A) and OCR (Figure 5B) remained invariant from baseline to interim and up to the end of the observation period. This finding apparently suggested the invariance of energy demand of PBMCs exposed to chemotherapy. However, this interpretation was challenged by the analysis of oxygen fate. Indeed, the mitochondrial oxygen usage progressively increased during the treatment in both its fractions (ATP-linked and ATP-independent) (Figure 5 C and D). Consequently, the OCR fraction accounted by nonmitochondrial usage showed a significant decrease at the interim evaluation that persisted thereafter (Figure 5E).

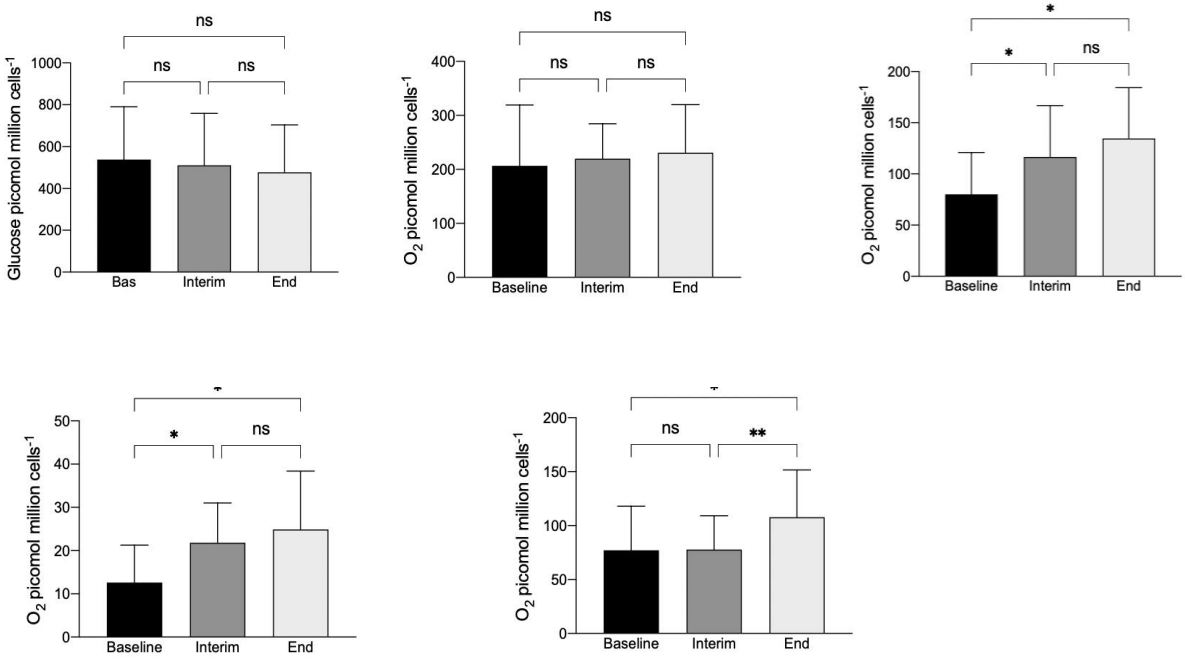

Figure 5 Chemotherapy and PBMCs energy metabolism results

In Figure 5A and 5B the graphs show that glucose consumption and OCR remained invariant from baseline to interim and up to the end of the observation period. This result seemingly indicated that the energy demand of PBMCs exposed to chemotherapy remained unchanged. Nonetheless, this interpretation was questioned by examining the fate of oxygen. In fact, mitochondrial oxygen consumption steadily increased during the treatment in both its ATP-linked and ATP-independent fractions (Figure 5 C and D). As a result, the OCR fraction attributed to non-mitochondrial consumption showed a significant decrease at the interim evaluation and continued to do so thereafter (Figure 5E).

3.4 PBMCs oxygen usage and response to chemotherapy

According to the Lugano criteria [28], 18 out of 23 (78%) patients showed a complete response to ABVD therapy and were thus defined as “responders”. Despite the similar Deauville score at interim study [32], the remaining five patients were classified as “non-responders”. No difference was observed in both age (54±18 vs 52±21 in non-responders vs responders, respectively, p=ns) or in female gender prevalence (40% vs 33%, respectively, ns).

Glucose consumption was not related to treatment effectiveness at any of the three studied time points (Figure 6A). By contrast, the OCR response to ABVD treatment (Figure 6B) was different in the two groups. It did not change in responders, while in non-responders it showed a progressive increase ($p<0.05$, at repeated measures one way ANOVA) and became significantly higher than in patients with complete remission, after the end of treatment (290±54 vs 211±90 picomol O_2 x min^{-1} x million $cells^{-1}$, respectively, $p<0.05$) (Figure 6B).

In non-responders patients, this behavior selectively involved the mitochondria, as both respiratory (ATP-linked) and ATP-independent (oligomycin insensitive) OCR progressively increased from baseline to interim and end-therapy (Figure 6C and D). By contrast, the non-mitochondrial (rotenone/antimycin insensitive) OCR fraction did not show significant differences between the two groups (Figure 6E). Finally, the different response of mitochondrial function was not related to any change in the PBMCs composition, as the monocytes/lymphocytes ratio was similar in the two groups at all studied time points (Figure 6F).

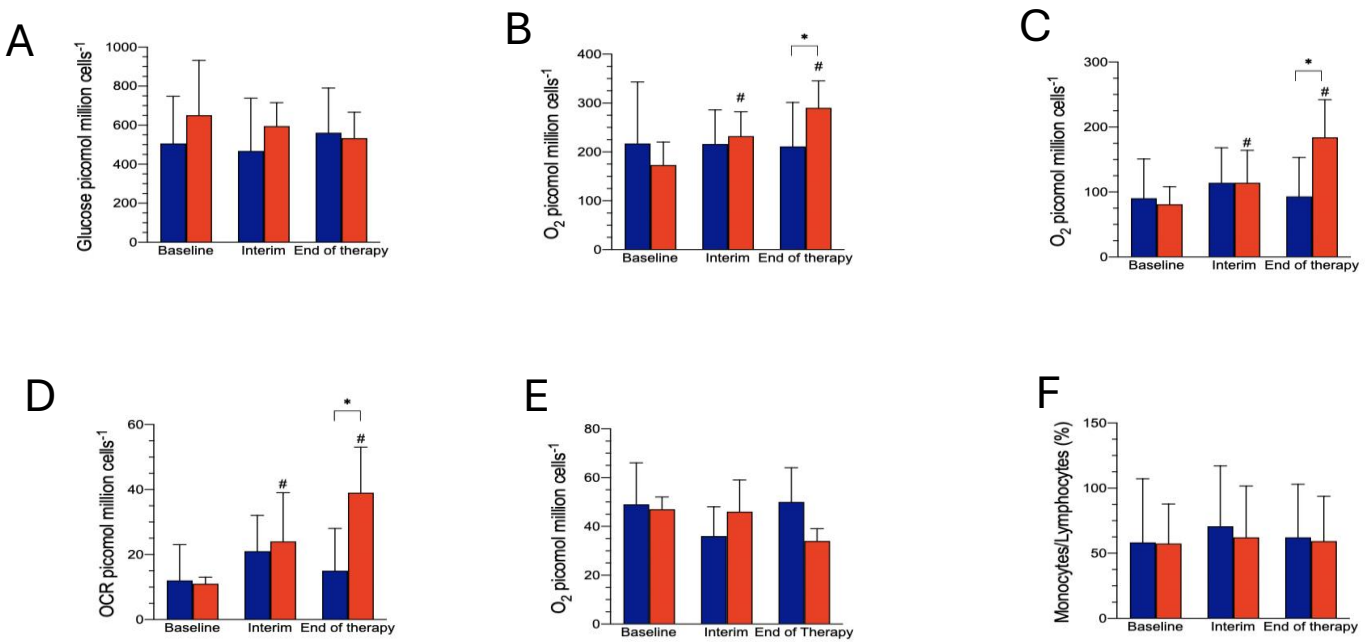

Figure 6 PBMCs oxygen usage and response to chemotherapy results

Patients underwent a PET/CT scan three months after the end of the treatment to determine their response to therapy. This allowed for distinguishing patients into responders and non-responders. Responders were characterized by the disappearance of lesions (in blue), while non-responders were characterized by the persistence of lesions (in red). According to the Lugano criteria], 18 out of 23 (78%) patients showed a complete response to ABVD therapy and were thus defined as "responders". Despite the similar Deauville score at interim study, the remaining five patients were classified as "non-responders". No difference was observed in both age (54±18 vs 52±21 in non-responders vs responders, respectively, p=ns) or in female gender prevalence (40% vs 33%, respectively, ns). Glucose consumption was unrelated to the effectiveness of the treatment at any of the three time points studied (Figure 6A). However, the OCR response to ABVD treatment (Figure 6B) differed between the two groups. It remained unchanged in responders, whereas it progressively increased in non-responders (p<0.05, at repeated measures one-way ANOVA) and became significantly higher than in patients who achieved complete remission after the end of treatment (290±54 vs 211±90 picomol O2 x min^-1 x million cells^-1, respectively, p<0.05) (Figure 6B).

In non-responders, this behavior was specifically related to the mitochondria, as both respiratory (ATP-linked) and ATP-independent (oligomycin-insensitive) OCR progressively increased from baseline to interim and end-therapy (Figure 6C and D). In contrast, the non-mitochondrial (rotenone/antimycin-insensitive) OCR fraction did not show significant differences between the two groups (Figure 6E). Finally, the differing response of mitochondrial function was not associated with any change in PBMC composition, as the monocyte/lymphocyte ratio was similar in both groups at all time points studied (Figure 6F).

3.5 Mitochondrial DNA analysis

Mitochondrial DNA copy number was not significantly different between control subjects and patients (Figure 7A). However, when the whole HL group was analyzed, mtDNA copy number was significantly increased at the interim time to come back to the baseline values at the end of treatment (Figure 7B). This effect was not caused by any variation in the cells populating the analyzed sample whose prevalence did not change at the three time points (Figure 7C). Similarly, mt-DNA copy number were largely independent of the ratio between monocytes and lymphocytes regardless the disease phase analyzed (Figure 7D). The response of MIT-DNA copy number was not homogeneously distributed in the studied HL patients. Indeed, after a similar increase at the interim phase, MIT-DNA copy number decreased back to the baseline values in the responders. By contrast, it remained elevated in non-responder patients (Figure 7E).

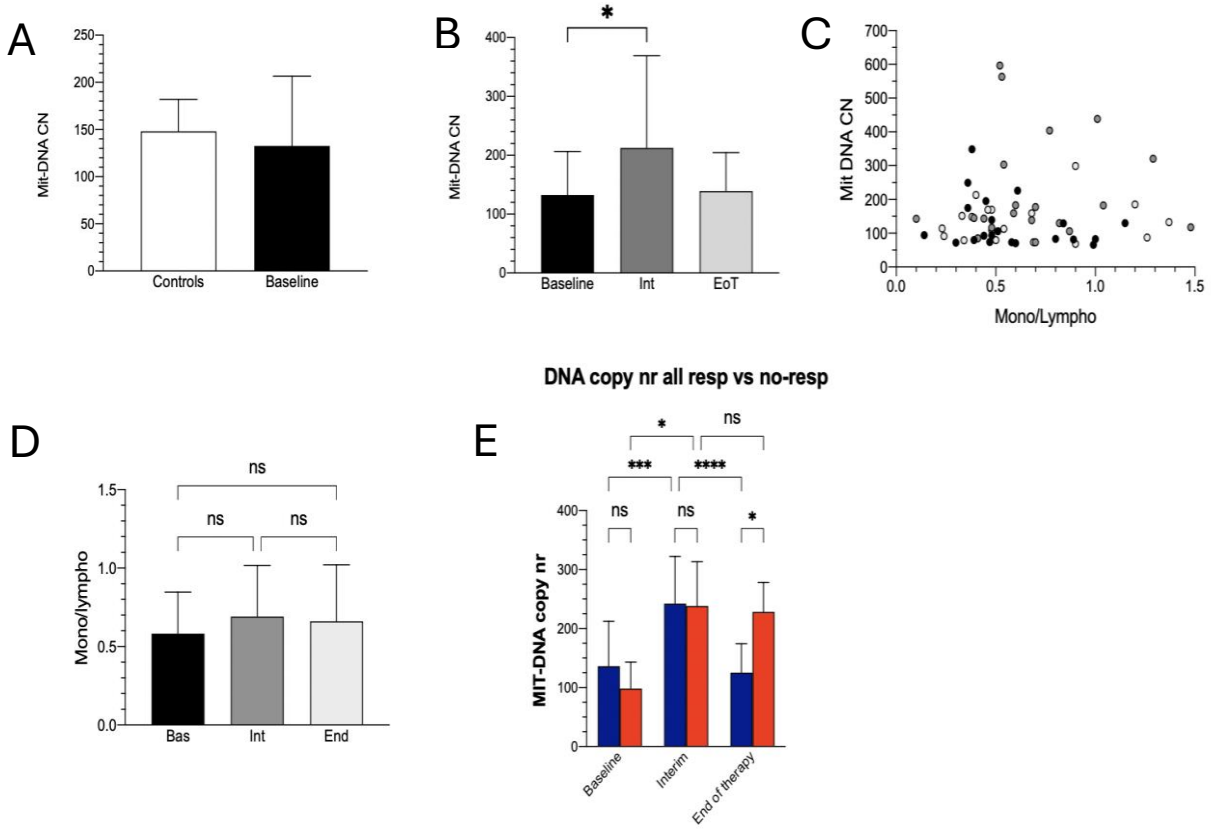

Figure 7 Mitochondrial DNA analysis

As seen in Figure 7A the mitochondrial DNA copy number did not differ significantly between control subjects and patients. However, in the overall HL group, the mtDNA copy number significantly increased at the interim time point and returned to baseline values by the end of treatment (Figure 7B). This change was not due to variations in the cell populations of the analyzed samples, as their prevalence remained constant across the three time points (Figure 7C). Similarly, mtDNA copy number was largely unaffected by the monocyte to lymphocyte ratio, regardless of the disease phase analyzed (Figure 7D). The response of mtDNA copy number was not uniform among the HL patients studied. After a similar interim increase, mtDNA copy number returned to baseline values in responders, while it remained elevated in non-responders (Figure 7E).

4. DISCUSSION

Analyzing the energy metabolism, we found that PBMCs harvested from HL patients are characterized by high rate of glucose degradation to lactate with respect to control ones. By contrast, although oxygen consumption is similar between PBMCs collected from control subjects and patients in basal conditions, the OCR mitochondrial fraction is significantly decreased in PBMCs of the latter. These data indicated a different metabolic reprogramming between the two populations studied, although there are not neoplastic cells involved. Furthermore, it must be underlined that this metabolic comparison was conducted between PBMCs taken from control subjects and patients not yet subjected to any therapy and that these patterns involve normal circulating cells virtually free from the contamination of neoplastic elements. Moreover, our results showed that, despite a normal density of mitochondria - as indexed by the mtDNA copy number - the high rate of glycolytic flux matches a decelerated function of these organelles as displayed by the low oxygen usage, in both its fractions (ATP-linked and ATP independent). Furthermore, the mtDNA copy number does not have stable coverage during the treatment of all HL patients. Indeed, mtDNA copies increase significantly after two cycles of therapy, in the so-called interim phase, to return to a level like baseline at the end of treatment. Finally, in responder patients, ABVD therapy induced an evident up and down pattern of mtDNA copy number. This trend was partially reproduced by OCR whose modifications, however, did not reach the statistical significance. The PBMCs of patients with disease persistence at the end of chemotherapy showed a different behavior: despite a similar response to the first ABVD cycles, their mitochondrial copy number did not come back to the baseline values and remained elevated at least up the late control late after treatment discontinuation. Again, this trend was partially reproduced by the respiratory function,

since both, ATP-related and ATP-independent, fractions of mitochondrial oxygen usage significantly increased from baseline to interim up to the end of therapy.

4.1 Metabolic asset in the studied populations.

The number of HL patients enrolled in the present study was relatively low. However, this limitation was motivated by the need to avoid the interference of any variation in the administered chemotherapy regimen on PBMCs metabolic features. Accordingly, the analysis was limited to those patients submitted to the same ABVD regimen for the whole observation period, from the staging up to the end of therapy. This selection criterion forced us to limit the enrollment according to a Deauville score at the interim evaluation ranging 1 to 3.

The large increase in glycolytic flux of HL patients compared with control subjects was not related to any bias related to age, according to by the case-control criterion used for the selection [33]. Similarly, it was not attributable to a significant difference in the composition of sampled PBMCs, since the relative prevalence of monocytes and lymphocytes were similar in the two groups at the baseline examination. Likewise, the different behavior of OCR and mtDNA copy number in responders and non-responder patients cannot be explained by a possible alteration of the PBMCS composition. Indeed, the ratio between monocytes and lymphocytes did not significantly change during the three time points, although monocyte prevalence showed a slight and not significant at the interim phase. Accordingly, the variation of mitochondrial number and respiratory function most likely reflects the metabolic response of studied cells to ABVD. This same response implied a progressive acceleration of mitochondrial number and respiratory activity in non-responders as opposed to responder ones whose PBMCs showed an only

transient increase in mtDNA copy number associated with a trivial and not significant alteration in mitochondrial OCR.

4.2 Mitochondrial asset and anthracycline toxicity

Several studies already evaluated the effect of anthracyclines on mitochondrial function and number. In agreement with our observation in normal PBMCs, an increase in mtDNA copy number has been found to predict the resistance against anthracycline toxicity of cultured cell lines derived from breast [34], head and neck or lung carcinomas [35].

Similarly, Kusao et al reported that a marked increase in mtDNA copy number identifies chemo-resistant cells harvested from pediatric patients treated with doxorubicin for Burkitt lymphoma [36]. Although the mechanisms underlying this response have not been fully elucidated, Malik et al proposed that the increased mtDNA asset might reflect an upregulated mitochondrial biogenesis in the presence of a high redox stress [37]. Similarly, the preliminary administration of dexrazoxane has been shown to almost fully prevent this response in a pediatric cohort of survivors after diagnosis of acute lymphoblastic leukemia [38]. The relevance of these in vitro studies has been verified in the clinical setting by Hsu and coworkers who documented that high mtDNA copy number in the surgical specimen is associated with a poor outcome in patients with breast cancer treated with anthracyclines [39]. The previously quoted studies focused on cancer, our approach aimed instead to characterize the metabolic effect of ABVD regimen on normal cells epitomized by the circulating PBMCs of HL patients. This decision was motivated by the notion that the mitochondrial function is a primary promoter of anthracycline toxicity on the myocardium [40]. Nevertheless, a relatively lower experience focused on the hypothesis that the cytotoxic effect of anthracyclines might

reflect the activation of the same mechanisms in cancer cells as in normal ones. Christensen et al reported an increased respiration coupled with an increase mtDNA copy number in the PBMCs harvested from patients treated with adjuvant therapy for an early-stage breast cancer [41]. Similarly, Qu et al already reported that a high mtDNA copy number in leucocytes populating the peripheral blood predicts a poor outcome in patients with colorectal carcinoma [42]. The present data extend this previous observation documenting that the anthracycline interference on mitochondrial balance is not limited to cancer and is rather shared with normal host cells. More importantly, the type of interference on normal cells predicts the therapy effectiveness on cancer lesions. Indeed, the PBMCs harvested from patients with persistent disease showed a progressive increase in mitochondrial OCR coupled with a persistent elevation of mitochondrial number.

5. CONCLUSIONS

The present data indicate that the therapeutic effectiveness of anthracyclines on HL is associated with a specific behavior of normal PBMCs whose mitochondrial copy number and function are restored to baseline values after the transient increase induced by chemotherapy. By contrast, the resistance to ABVD treatment is associated with a progressive acceleration of mitochondrial function and mtDNA copy number that persists after treatment discontinuation. Previous studies already suggested the cancer and its generating ecosystem (the host) share a similar response to anthracycline toxicity. The present study extends this notion by showing that this sharing involves the regulation of mitochondrial function and biogenesis, identifying the analysis of PBMCs as a possible marker of treatment effectiveness, at least in HL patients.

BIBLIOGRAPHY

1. J. Momotow et al. “Hodgkin Lymphoma—Review on Pathogenesis, Diagnosis, Current and Future Treatment Approaches for Adult Patients” Journal of clinical medicine 2021
2. D. A. G. van Bladel et al. “Novel Approaches in Molecular Characterization of Classical Hodgkin Lymphoma” Cancers 2022
3. R. T. Hoppe et al. “Hodgkin Lymphoma, version 2.2020, NCCN Clinical Practice Guidelines in Oncology” Journal of the National Comprehensive Cancer Network 2020
4. S. Ramos et al. “Characterizing Chemotherapy/Radiotherapy- Induce Genome Chaos In Hodgkin’s Lymphoma Patients Using M-FISH” Methods in molecular biology 2024
5. B. D. Cheson et al. “Recommendations for Initial Evaluation, Staging, and Response Assessment of Hodgkin and Non-Hodgkin Lymphoma: The Lugano Classification” Journal of clinical oncology 2014
6. C. Marini et al. “Myocardial Metabolic Response Predicts Chemotherapy Curative Potential on Hodgkin Lymphoma: A Proof-of-Concept Study” Biomedicines 2021
7. Kamińska K, Cudnoch-Jędrzejewska A. A Review on the Neurotoxic Effects of Doxorubicin. Neurotox Res. 2023
8. Mohan UP, P B TP, Iqbal STA, Arunachalam S. Mechanisms of doxorubicin-mediated reproductive toxicity - A review. Reprod Toxicol. 2021
9. K. Renu et al. “Toxic effects and molecular mechanism of doxorubicin on different organs – an update” Taylor and Francis 2020
10. TOKARSKA -SCHLATTNER M, DOLDER M, G ERBER I et al. Reduced creatine-stimulated respiration in doxorubicin challenged mitochondria: particular sensitivity of the heart.Biochim Biophys Acta 2007
11. Lebrecht D, Setzer B, Ketelsen UP, Haberstroh J, Walker UA.Time-dependent and tissue-specific accumulation of mtDNA andrespiratory chain defects in chronic doxorubicin cardiomyopathy.Circulation 2003
12. Deng S, Kruger A, Kleschyov AL, Kalinowski L, Daiber A, Wojnowski L. Gp91phox-containing NAD(P)H oxidase increases superoxide formation by doxorubicin and NADPH. Free Radic Biol Med. 2007;
13. Huang J, Wu R, Chen L, Yang Z, Yan D, Li M. Understanding Anthracycline Cardiotoxicity From Mitochondrial Aspect. Front Pharmacol. 2022
14. Lebrecht D, Kokkori A, Ketelsen UP, Setzer B, Walker UA. Tissue-specific mtDNA lesions and radicalassociated mitochondrial dysfunction in human hearts exposed to doxorubicin. J Pathol. 2005
15. C. A. Castellani et al. “Thinking outside the nucleus: Mitochondrial DNA copy number in health and disease” Mitochondrion 2020
16. Z. Rong et al. “The Mitochondrial Response to DNA” Frontiers in cell and developmental biology 2021
17. M. Alexeyev et al. “The Maintenance of Mitochondrial DNA Integrity-Critical Analysis and Update” Cold Spring Harbor Perspectives in biology 2013
18. T. Khan et al. “Mitochondrial Dysfunction: Pathophysiology and Mitochondria-Targeted Drug Delivery Approaches” Pharmaceutics 2022
19. M. Yu “Generation, function and diagnostic value of mitochondrial DNA copy number alterations in human cancers” Life Science 2011

20. C. A. Castellani et al. “Mitochondrial DNA copy number can influence mortality and cardiovascular disease via methylation of nuclear DNA CpGs” Genome Medicine 2020
21. Q. Lan et al “A prospective study of mitochondrial DNA copy number and risk of non-Hodgkin lymphoma” Blood 2008
22. I. Kusao et al. “Chemotoxicity recovery of mitochondria in non-Hodgkin lymphoma resulting in minimal residual disease” Pediatric Blood Cancer 2008
23. X. He et al. “High leukocyte mtDNA content contributes to poor prognosis through ROS-mediated immunosuppression in hepatocellular carcinoma patients.” Oncotarget 2016
24. L. Hu et al. “Altered mitochondrial DNA copy number contributes to human cancer risk: Evidence from an updated meta-analysis” Scientific reports 2016
25. Mohd Khair S.Z.N., Abd Radzak S.M., Mohamed Yusoff A.A. The Uprising of Mitochondrial DNA Biomarker in Cancer. Dis. Markers. 2021
26. Hoppe R.T., Advani R.H., Ai W.Z., Ambinder R.F., Armand P., Bello C.M., Benitez C.M., Bierman P.J., Boughan K.M., Dabaja B., et al. Hodgkin Lymphoma, Version 2.2020, NCCN Clinical Practice Guidelines in Oncology. J. Natl. Compr. Cancer Netw. 2020
27. Biggi A, Chauvie S, Fallanca F, Guerra L, Bergesio F, Menga M, Bianchi A, Gregianin M, Chiaravalloti A, Schillaci O, Pavoni C, Patti C, Picardi M, Romano A, Schiavotto C, Sorasio R, Viviani S, La Nasa G, Trentin L, Rambaldi A, Gallamini A. Predictive value on advance hodgkin lymphoma treatment outcome of end-of treatment FDG PET/CT in the HD0607 clinical trial. Hematol Oncol. 2023.
28. Cheson BD, Fisher RI, Barrington SF, Cavalli F, Schwartz LH, Zucca E, Lister TA; Alliance, Australasian Leukaemia and Lymphoma Group; Eastern Cooperative Oncology Group; European Mantle Cell Lymphoma Consortium; Italian Lymphoma Foundation; European Organisation for Research; Treatment of Cancer/Dutch Hemato-Oncology Group; Grupo Español de Médula Ósea; German High-Grade Lymphoma Study Group; German Hodgkin's Study Group; Japanese Lymphorra Study Group; Lymphoma Study Association; NCIC Clinical Trials Group; Nordic Lymphoma Study Group; Southwest Oncology Group; United Kingdom National Cancer Research Institute. Recommendations for initial evaluation, staging, and response assessment of Hodgkin and non-Hodgkin lymphoma: the Lugano classification. J Clin Oncol. 2014
29. Carta S., Penco F., Lavieri R., Martini A., Dinarello C.A., Gattorno M., Rubartelli A. Cell stress increases ATP release in NLRP3 inflammasome-mediated autoinflammatory diseases, resulting in cytokine imbalance. Proc. Natl. Acad. Sci. USA. 2015
30. Jones N., Piasecka J., Bryant A.H., Jones R.H., Skibinski D.O., Francis N.J., Thornton C.A. Bioenergetic analysis of human peripheral blood mononuclear cells. Clin. Exp. Immunol. 2015
31. Anna Truini et al. “Downregulation of miR-99a-let-7c/miR-125b miRNA cluster predicts clinical outcome in patients with unresected malignant pleural mesothelioma” Oncotarget 2017
32. Meignan M, Gallamini A, Haioun C. Report on the First International Workshop on Interim-PET-Scan in Lymphoma. Leuk Lymphoma. 2009
33. Wong J, McLennan SV, Molyneaux L, Min D, Twigg SM, Yue DK. Mitochondrial DNA content in peripheral blood monocytes: relationship with age of diabetes onsetand diabetic complications. Diabetologia. 2009

34. Zhuang F, Huang S, Liu L. PYCR3 modulates mtDNA copy number to drive proliferation and doxorubicin resistance in triple-negative breast cancer. Int J Biochem Cell Biol. 2024 Jun;171:106581. doi: 10.1016/j.biocel.2024.106581. Epub 2024
35. Mei H, Sun S, Bai Y, Chen Y, Chai R, Li H. Reduced mtDNA copy number increases the sensitivity of tumor cells to chemotherapeutic drugs. Cell Death Dis. 2015
36. Kusao I, Agsalda M, Troelstrup D, Villanueva N, Shiramizu B. Chemotoxicity recovery of mitochondria in non-Hodgkin lymphoma resulting in minimal residual disease. Pediatr Blood Cancer. 2008
37. Malik F, Kumar A, Bhushan S, Khan S, Bhatia A, Suri KA, Qazi GN, Singh J. Reactive oxygen species generation and mitochondrial dysfunction in the apoptotic cell death of human myeloid leukemia HL-60 cells by a dietary compound withaferin A with concomitant protection by N-acetyl cysteine. Apoptosis. 2007
38. Lipshultz SE, Anderson LM, Miller TL, Gerschenson M, Stevenson KE, Neuberg DS, Franco VI, LiButti DE, Silverman LB, Vrooman LM, Sallan SE; Dana-Farber Cancer Institute Acute Lymphoblastic Leukemia Consortium. Impaired mitochondrial function is abrogated by dexrazoxane in doxorubicin-treated childhood acute lymphoblastic leukemia survivors. Cancer. 2016
39. Hsu CW, Yin PH, Lee HC, Chi CW, Tseng LM. Mitochondrial DNA content as a potential marker to predict response to anthracycline in breast cancer patients. Breast J. 2010 May-Jun;16(3):264-70. doi: 10.1111/j.1524-4741.2010.00908.x. Epub 2010
40. Yin J, Guo J, Zhang Q, Cui L, Zhang L, Zhang T, Zhao J, Li J, Middleton A, Carmichael PL, Peng S. Doxorubicin-induced mitophagy and mitochondrial damage is associated with dysregulation of the PINK1/parkin pathway. Toxicol In Vitro. 2018 Sep;51:1-10. doi: 10.1016/j.tiv.2018.05.001. Epub 2018
41. Christensen IB, Abrahamsen ML, Ribas L, Buch-Larsen K, Marina D, Andersson M, Larsen S, Schwarz P, Dela F, Gillberg L. Peripheral blood mononuclear cells exhibit increased mitochondrial respiration after adjuvant chemo- and radiotherapy for early breast cancer. Cancer Med. 2023
42. Qu F, Chen Y, Wang X, He X, Ren T, Huang Q, Zhang J, Liu X, Guo X, Gu J, Xing J. Leukocyte mitochondrial DNA content: a novel biomarker associated with prognosis and therapeutic outcome in colorectal cancer. Carcinogenesis. 2015

RINGRAZIAMENTI

A Mamma e Papà,

Al vostro coraggio e ai vostri sacrifici,

Alla vostra forza e alla vostra umiltà.

Ogni mio traguardo

È riflesso del vostro amore.

A Francesco,

alla tua anima pura,

al tuo cuore immenso,

e all'amore incondizionato.

Con te,

ciò che era spigolo,

è diventato cerchio perfetto.

Ce l'abbiamo fatta!

Agli amici del cuore,

Quelli di sempre e quelli nuovi,

Con l'augurio di avervi sempre con me.

Al mio relatore, Dott. Gianmario Sambuceti e alla Dott.ssa Cecilia Marini, grazie per avermi trasmesso ogni giorno l'immensa passione per il vostro lavoro e di aver creduto in me ancora prima di conoscermi, siete fonte di ispirazione e un esempio da seguire.

Ma soprattutto, Grazie a Sabrina, alla tua pazienza e alla tua dolcezza, sei stata insegnante e amica. Hai dimostrato, al di là dei doveri accademici, cosa significhi essere un vero mentore, lasciandomi insegnamenti che mi accompagneranno sempre.